



# Multiparametric Strategy to Predict Early Disease Decompensation in Asymptomatic Severe Aortic Regurgitation

Radka Kočková<sup>1</sup> MD, PhD; Hana Línková, MD; Zuzana Hlubočká<sup>2</sup> MD, PhD; Karel Mědílek, MD; Martin Tuna<sup>3</sup> MD, PhD; Jan Vojáček, MD, PhD; Ivo Skalský, MD, PhD; Štěpán Černý MD, PhD; Jiří Malý, MD, PhD; Jaroslav Hlubočký, MD, PhD; Takuya Mizukami<sup>4</sup> MD, PhD; Cristina De Colle, MD; Martin Pěnička, MD, PhD

**BACKGROUND:** Use of the current echocardiography-based indications for aortic regurgitation (AR) surgery might result in late valve replacement at the stage of irreversible myocardial damage. Therefore, we aimed to identify simple models combining multiple echocardiography or magnetic resonance imaging (MRI)-derived indices and natriuretic peptides (BNP [brain natriuretic peptide] or NT-proBNP [N-terminal pro-B type natriuretic peptide]) to predict early disease decompensation in asymptomatic severe AR.

**METHODS:** This prospective and multicenter study included asymptomatic patients with severe AR, preserved left ventricular ejection fraction (>50%), and sinus rhythm. The echocardiography and MRI images were analyzed centrally in the CoreLab. The study end point was the onset of indication for aortic valve surgery as per current guidelines.

**RESULTS:** The derivative cohort consisted of 127 asymptomatic patients (age 45±14 years, 84% males) with 41 (32%) end points during a median follow-up of 1375 (interquartile range, 1041–1783) days. In multivariable Cox regression analysis, age, BNP, 3-dimensional vena contracta area, MRI left ventricular end-diastolic volume index, regurgitant volume, and a fraction were identified as independent predictors of end point (all  $P<0.05$ ). However, a combined model including one parameter of AR assessment (MRI regurgitant volume or regurgitant fraction or 3-dimensional vena contracta area), 1 parameter of left ventricular remodeling (MRI left ventricular end-diastolic volume index or echocardiography 2-dimensional global longitudinal strain or E wave), and BNP showed significantly higher predictive accuracy (area under the curve, 0.74–0.81) than any parameter alone (area under the curve, 0.61–0.72). These findings were confirmed in the validation cohort ( $n=100$  patients, 38 end points).

**CONCLUSIONS:** In asymptomatic severe AR, multimodality and multiparametric model combining 2 imaging indices with natriuretic peptides, showed high accuracy to identify early disease decompensation. Further prospective studies are warranted to explore the clinical benefit of implementing these models to guide patient management.

**REGISTRATION:** URL: <https://www.clinicaltrials.gov>; Unique identifier: NCT02910349

**GRAPHIC ABSTRACT:** A graphic abstract is available for this article.

**Key Words:** aortic valve ■ echocardiography ■ magnetic resonance imaging ■ natriuretic peptide, brain ■ prognosis

## See Editorial by Fontana and Ioannou

**A**ortic regurgitation (AR) is the third most common<sup>1–6</sup> valvular heart disease affecting mainly younger males.<sup>1,4</sup> Severe chronic AR may be clinically silent for a long time but eventually leads to heart failure with

reduced life expectancy.<sup>1,3,7</sup> It is of note that even before the onset of symptoms or left ventricular (LV) decompensation, severe AR is associated with increased annual mortality.<sup>7–9</sup> This suggests relative insensitivity of current

Correspondence to: Radka Kočková MD, PhD, Center for Congenital Heart Disease in Adults, Na Homolce Hospital, Cardiothoracic Surgery Department, Roentgenova 37/2, Prague, 15030. Email [radka.kockova@centrum.cz](mailto:radka.kockova@centrum.cz)

Supplemental Material is available at <https://www.ahajournals.org/doi/suppl/10.1161/CIRCIMAGING.122.014901>.

Continuing medical education (CME) credit is available for this article. Go to <http://cme.ahajournals.org> to take the quiz.

For Sources of Funding and Disclosures, see page 908.

© 2022 American Heart Association, Inc.

Circulation: Cardiovascular Imaging is available at [www.ahajournals.org/journal/circimaging](http://www.ahajournals.org/journal/circimaging)

## CLINICAL PERSPECTIVE

The optimal timing of surgical treatment in asymptomatic patients with chronic severe aortic regurgitation remains challenging. A current approach integrating symptoms, echocardiography-derived aortic regurgitation assessment, and left ventricular remodeling is rather insensitive to detect ongoing myocardial damage and the need for early aortic valve intervention. In the present study of 127 patients the age, serum level of brain natriuretic peptide, echocardiography-derived 3-dimensional vena contracta area, magnetic resonance–derived left ventricular end-diastolic volume index, regurgitant volume and fraction were independent predictors of early disease progression leading aortic valve surgery. However, a multiparametric model combining markers of (1) aortic regurgitation severity, (2) a marker of left ventricular remodeling, and (3) brain natriuretic peptide serum level, showed higher predictive accuracy than any parameter alone. A comprehensive examination of asymptomatic patients with moderate to severe chronic aortic regurgitation using echocardiography, cardiac magnetic resonance, and serum brain natriuretic peptide might be useful. The presented multiparametric model helps to identify patients with a high likelihood of early disease progression and aortic valve surgery. However, further clinical studies are warranted to show if early surgery will result in a better outcome in asymptomatic patients with chronic severe aortic regurgitation and a high risk of early disease progression.

## Nonstandard Abbreviations and Acronyms

|             |                            |
|-------------|----------------------------|
| <b>AR</b>   | aortic regurgitation       |
| <b>BNP</b>  | brain natriuretic peptide  |
| <b>ECV</b>  | extracellular volume       |
| <b>EDVI</b> | end-diastolic volume index |
| <b>EF</b>   | ejection fraction          |
| <b>ESVI</b> | end-systolic volume index  |
| <b>LV</b>   | left ventricle             |
| <b>MRI</b>  | magnetic resonance imaging |
| <b>RF</b>   | regurgitant fraction       |
| <b>RV</b>   | regurgitant volume         |

guidelines triggers for early aortic valve (AV) intervention.<sup>10–12</sup> Moreover, a non-negligible number of patients undergoing AV surgery have already irreversible myocardial damage with a negative impact on their long-term outcome.<sup>10,13</sup> However, perioperative mortality has decreased with novel surgical techniques and perioperative care.<sup>8,9,11</sup> However, the clinical decision of whether or not to indicate early AV intervention remains challenging.

Cardiac magnetic resonance imaging (MRI) is an accurate and reproducible technique to assess aortic

flow and LV remodeling.<sup>6,14</sup> In asymptomatic patients with preserved LV ejection fraction (EF), we have observed high accuracy of the MRI-derived quantification of AR to identify individuals in need of early AV surgery.<sup>15</sup> However, a multiparametric strategy involving not only AR quantification but also an assessment of LV remodeling, natriuretic peptides, or different imaging modalities may be more accurate to guide clinical decisions toward early AV intervention. Therefore, the present study aimed to identify simple models including multiple echocardiographic or MRI-derived indices and natriuretic peptides to predict early disease decompensation in asymptomatic patients with severe AR and preserved LV EF. The accuracy of these models was tested in an external validation cohort.

## METHODS

Deidentified data on which this work is based will be available, they can be requested from the corresponding author, upon reasonable request.

### Design

The study was a prospective, multicenter, and observational, conducted in six tertiary centers (5 derivation cohorts in the Czech Republic, and 1 external validation cohort in Belgium). In the derivative cohort, analysis of all the echocardiographic and MRI images was performed in a CoreLab located in one of the tertiary cardiology centers (Institute for Clinical and Experimental Medicine, Prague), which is the holder of the European Association of Cardiovascular Imaging Laboratory accreditation for advanced echocardiography. The MRI images were analyzed by a physician holding a European Association of Cardiovascular Imaging Level 3 Diploma in Cardiovascular MRI. The readers were blinded to all other data and outcomes. In the validation cohort, the echocardiography and MRI imaging were performed and analyzed in the Cardiovascular Center Aalst.

### Patients

The derivative cohort consisted of consecutive asymptomatic patients ( $n=127$ , age  $45\pm 14$  years, 84% males) with isolated severe AR referred to all 5 participating centers for AR assessment between March 2015 and May 2019. As per study protocol,<sup>15</sup> only adult patients in sinus rhythm with LV EF  $>50\%$ , LV end-diastolic diameter  $\leq 70$  mm, and LV end-systolic diameter  $\leq 25$  mm/m<sup>2</sup> with a single valve lesion were included. Patients with poor echocardiographic image quality, contraindications for MRI, or severe comorbidities limiting life expectancy ( $<3$  years) were excluded. The severity of AR was established utilizing an integrative echocardiographic approach according to the American Society of Cardiology and European Association of Cardiovascular Imaging recommendations.<sup>14</sup> The absence of symptoms was validated using exercise testing. The validation cohort consisted of consecutive asymptomatic patients ( $n=100$ , age  $46\pm 15$  years, 82% males) included in the Cardiovascular Center Aalst according to the same eligibility criteria. The study protocol and informed consent were approved by the Ethics committees in all participating centers.<sup>15</sup>

## Study Protocol

At baseline, all patients underwent comprehensive 2-dimensional (2D) and 3D echocardiography, exercise testing, and blood sample analysis in the participating centers. All MRI examinations were performed in a single center where the CoreLab was located. A total of 60 (47%) patients underwent MRI on the same day as baseline echocardiography while the remaining patients were referred for MRI within 2 weeks after enrollment. During the follow-up, every 6 months the clinical, biochemical, and echocardiographic data were recorded in each participating center. The decision about further patient management was left to the experienced heart valve team in the particular center. The follow-up data on AV surgery, hospitalization, and mortality were obtained using the hospital database and population registry.

Study end point was the onset of indication for AV surgery as per current guidelines.<sup>1</sup>

## Echocardiography

A comprehensive 2D and 3D echocardiography was performed using Vivid 7, Vivid E9, and Vivid E95 (GE Healthcare, Horten, Norway) ultrasound system according to the study protocol described in detail previously.<sup>15</sup> Blood pressure and heart rate were recorded during examination in all patients. At least 3 R-R loops were recorded for each meticulously optimized view, digitally stored, and analyzed offline in the CoreLab. The average measurements from all 3 loops were databased.

## Grading of AR Severity

The AR severity was graded utilizing recommended algorithm of the American Society of Cardiology integrating qualitative, semiquantitative, and quantitative measures.<sup>14</sup> The only deviation from this algorithm was in quantitative measurement as the majority of included patients (n=95; 74.8%) had other than a 3-cusp aortic valve with eccentric or multiple jets. A flow convergence method is less accurate in this setting; thus, the stroke volume measurement of regurgitant volume (RV) and a regurgitant fraction (RF) was preferred. In brief, the left ventricular outflow tract area was measured using 3D echocardiography at the annulus during systole and the mitral annulus was measured using 2D echocardiography in 2 perpendicular planes in mid-diastole. The pulsed-wave Doppler signal was recorded at the same level of left ventricular outflow tract and mitral annulus. The RV of AR was calculated from the following equation:  $RV = Stroke\ volume_{LVOT} - Stroke\ volume_{Mitral\ annulus}$ .<sup>14</sup> Severe AR was defined by the presence of  $\geq 4$  of the following criteria: flail leaflet, VC width  $>6$  mm, jet width  $\geq 65\%$  of left ventricular outflow tract, large flow convergence, pressure-half-time  $<200$  ms, prominent holodiastolic flow reversal in the descending aorta, and dilated LV with normal function, RV  $\geq 60$  mL, and RF  $\geq 50\%$ .

Cardiac MRI was performed on a 1.5 Tesla scanner (Magnetom Avanto fit, Siemens). Blood pressure and heart rate were recorded during each examination. A blood sample for hematocrit assessment, needed for extracellular volume calculation (ECV), was drawn just before the examination. All dynamic scans were performed during a breath-hold lasting 10 to 20 s with retrospective electrocardiography-gating. Left ventricular volumes and EF were calculated in a CoreLab

using a stack of short-axis steady-state free precession cine sequences (8 mm slice thickness, 0 mm gap) with a thorough correction for the valve position utilizing commercially available software (Segment CMR, Medviso AB 2018, Sweden). Through-plane phase-contrast velocity mapping scans (6 mm slice thickness, 0 mm gap) were performed according to study protocol<sup>15</sup> meticulously perpendicular to blood flow at several levels of the aortic root aiming to be as close as 5 mm above the tips of valve leaflets in systole but avoiding the turbulence. Background velocity offset errors were corrected using the stationary phantom and post-processing correction using software Segment CMR before forward and backward flow calculations. RV and fraction were averaged from 3 measurements. A single breath-hold electrocardiography-triggered phase-sensitive inversion recovery gradient echo sequence was utilized for late gadolinium enhancement 8 to 15 minutes after administration of 0.19 mL/kg of 1-molar gadolinium-based contrast agent (Gadobutrol, GadovistW, Byer, Germany). Modified Look-Locker Inversion recovery sequence (field of view 360×301 mm, matrix 118×256, slice thickness 8 mm, voxel size 1.4 mm×1.4 mm×8 mm, echo time 1.1 ms, repetition time 359 ms, flip angle 35°, bandwidth 1.085 Hz/Pixel) was acquired in basal-to-mid LV short-axis sequence before and 15 minutes after contrast administration for native T1 relaxation time and ECV calculation. A detailed description of the study protocol was published previously.<sup>15,16</sup> The normal value for native T1 relaxation time on the same scanner is 980±22 ms.

## Statistical Analysis

Normality distribution of continuous variables was assessed visually with histograms and with the Shapiro-Wilk test. Continuous variables were summarized by using the mean and SD or the median and interquartile range. Categorical variables were presented as frequency counts and percentages. Fisher exact test was used to compare 2 categorical variables, while the Mann-Whitney *U* test was performed for the comparison of 2 continuous ones. Correlation between variables was assessed by Pearson or Spearman test as appropriate. The hazard function was plotted by using spline regression for MRI-derived RV, MRI-derived RF, MRI-derived LV end-diastolic volume index, 3D echocardiography vena contracta area (3D VCA), echocardiography-derived LV global longitudinal strain (GLS), BNP (brain natriuretic peptide), to assess the appropriate GWI cut off points (hazard ratio, 1) for study end point. The Kaplan-Meier analysis and the Log-rank test were used to compare the cumulative incidence of the time-dependent binomial end points between patients with lower and higher MRI-derived RV, MRI-derived RF, MRI-derived LV end-diastolic volume index, BNP, 3D VCA, and transmitral E wave. Cox proportional hazard regression method was used to test the association between baseline variables and end point; results are presented as hazard ratio (95% CI). Proportional hazard assumptions were assessed by Schoenfeld residuals. Univariable and multivariable ROC curves were constructed to derive the area under the curve (AUC) of baseline variables to predict the end point. The backward selection procedure was used for building all multivariate models. The predictive accuracy of these models was tested on an external validation cohort. All statistical tests were considered significant at the  $P < 0.05$  level. All analyses were performed using the Statistical Package for Social Sciences,

version 25.0 (SPSS, PC version, Chicago, IL) or R software, version 3.6.1 (R Project for Statistical Computing).

blood pressure and heart rate between the echocardiography and MRI examinations.

## RESULTS

### Baseline Characteristics

Baseline clinical and imaging characteristics are shown in Tables 1 and 2, respectively. The study sample consisted of 127 patients (age 45±14 years, 84% males). All patients enrolled in the study were asymptomatic, in sinus rhythm, and with preserved LV EF. Using the echocardiography-derived integrative approach, all patients had severe AR, that is, grade III and IV, respectively, in 68 (54%) and 59 (46%) individuals. The cause of AR was a congenitally abnormal bicuspid valve in the majority of patients (n=90; 71%). Four (3%) patients had a history of coronary artery disease. Almost half of the individuals (49%) had hypertension. There were no significant differences in

### Clinical Outcome

During a median follow-up of 1375 (interquartile range, 1041–1783) days, a new indication for AV surgery, that is, study end point, was documented in 41 (32%) participants. The indication for AV surgery was onset of symptoms (n=34; 83%) and LV systolic dysfunction (n=7; 17%). Frequent ventricular ectopy leading to the deterioration of LV function developed in 2 patients. Individuals with versus without end point tended to be older ( $P=0.10$ ) and were more frequently using thiazide diuretics ( $P=0.0264$ ). All remaining clinical characteristics including medication were similar (Table 1). Patients with end point showed more advanced LV remodeling as documented by significantly higher BNP, larger LV end-diastolic diameter at echocardiography, LV volumes, and LV mass at MRI (all  $P<0.05$ ). In contrast, LV EF and

**Table 1. Baseline Clinical Characteristics**

|                                 | Total (n=127) | – End point (n=86) | + End point (n=41) | P value |
|---------------------------------|---------------|--------------------|--------------------|---------|
| Age, y                          | 45±14         | 44±14              | 49±14              | 0.10    |
| Male sex, N (%)                 | 107 (84)      | 73 (85)            | 34 (83)            | 0.78    |
| Hypertension, N (%)             | 60 (47)       | 38 (45)            | 22 (54)            | 0.42    |
| Diabetes, N (%)                 | 6 (5)         | 5 (6)              | 1 (2)              | 0.78    |
| Hyperlipidemia, N (%)           | 34 (27)       | 23 (27)            | 11 (26)            | 1.00    |
| Smoker, N (%)                   | 20 (16)       | 16 (19)            | 4 (10)             | 0.20    |
| Coronary artery disease, N (%)  | 4 (3)         | 3 (3)              | 1 (2)              | 1.00    |
| Previous cardiac surgery, N (%) | 4 (3)         | 4 (5)              | 0 (0)              | 0.30    |
| Stroke, N (%)                   | 2 (2)         | 1 (1)              | 1 (2)              | 1.00    |
| Aspirin, N (%)                  | 13 (10)       | 9 (11)             | 4 (10)             | 1.00    |
| Oral anticoagulants, N (%)      | 7 (6)         | 4 (5)              | 3 (7)              | 0.69    |
| ACE inhibitors/ARBs, N (%)      | 63 (50)       | 41 (48)            | 22 (54)            | 0.59    |
| Beta-blockers, N (%)            | 31 (24)       | 21 (24)            | 10 (24)            | 1.00    |
| Calcium channel blockers, N (%) | 23 (18)       | 12 (14)            | 11 (26)            | 0.14    |
| Thiazide diuretics, N (%)       | 17 (13)       | 7 (8)              | 10 (23)            | 0.0264  |
| Statins, N (%)                  | 25 (19)       | 15 (17)            | 10 (23)            | 0.48    |
| Height, cm                      | 180±9         | 180±8              | 179±9              | 0.44    |
| Weight, kg                      | 85±14         | 84±14              | 85±13              | 0.58    |
| Systolic blood pressure, mm Hg  | 135±17        | 134±16             | 138±17             | 0.14    |
| Diastolic blood pressure, mm Hg | 71±12         | 72±11              | 68±13              | 0.09    |
| Heart rate, bpm                 | 66±14         | 65±15              | 63±11              | 0.34    |
| Sinus rhythm, N (%)             | 127 (100)     | 86 (100)           | 41 (100)           | 1.00    |
| Serum creatinine, μmol/L        | 86±17         | 86±16              | 87±18              | 0.85    |
| <b>Aortic valve morphology</b>  |               |                    |                    |         |
| Trileaflet, N (%)               | 21 (17)       | 13 (15)            | 8 (20)             | 0.15    |
| Bicuspid, N (%)                 | 90 (71)       | 65 (76)            | 25 (61)            |         |
| Unicuspid/quadricuspid, N (%)   | 5 (4)         | 4 (5)              | 1 (2)              |         |
| Unknown, N (%)                  | 11 (9)        | 4 (5)              | 7 (16)             |         |

Values are means±SDs, median (interquartile range), or numbers (percentage). ACE/ARBs indicates angiotensin-converting enzyme/angiotensin receptor blockers.

**Table 2. Baseline Imaging Characteristics**

|  | Total (n=127) | – End point (n=86) | + End point (n=41) | P value |
|--|---------------|--------------------|--------------------|---------|
| <b>LV assessment</b>                                   |               |                    |                    |         |
| B-natriuretic peptide, ng/L                            | 67 (119)      | 43 (65)            | 117 (42)           | <0.001  |
| 2D ECHO end-diastolic diameter, mm                     | 58±6          | 57±6               | 60±6               | 0.0418  |
| 2D ECHO end-systolic diameter, mm                      | 37±5          | 36±5               | 38±6               | 0.16    |
| 2D ECHO end-systolic diameter index, mm/m <sup>2</sup> | 18±3          | 18±3               | 18±3               | 0.29    |
| 3D ECHO end-diastolic volume, mL                       | 174±50        | 168±40             | 179±54             | 0.08    |
| 3D ECHO end-diastolic volume index, mL/m <sup>2</sup>  | 83±25         | 81±23              | 86±23              | 0.18    |
| 3D ECHO end-systolic volume, mL                        | 67±24         | 65±20              | 65±28              | 0.10    |
| 3D ECHO end-systolic volume index, mL/m <sup>2</sup>   | 32±11         | 31±10              | 31±12              | 0.32    |
| 3D ECHO ejection fraction, %                           | 62±5          | 62±6               | 62±6               | 0.81    |
| 2D ECHO global longitudinal strain, %                  | 19±3          | 19±2               | 18±2               | 0.07    |
| Transmitral E wave velocity, cm/s                      | 66±17         | 68±17              | 60±14              | 0.0263  |
| Transmitral E/A wave ratio                             | 1.2±0.5       | 1.2±0.7            | 1.1±0.4            | 0.0289  |
| Septal annular e', cm/s                                | 9±3           | 9±3                | 9±3                | 0.65    |
| Lateral annular e', cm/s                               | 12±4          | 12±4               | 11±4               | 0.30    |
| E/e' ratio   | 9±3           | 7±3                | 8±3                | 0.67    |
| MRI end-diastolic volume, mL                           | 237±64        | 217±70             | 268±71             | <0.001  |
| MRI end-diastolic volume index, mL/m <sup>2</sup>      | 116±29        | 108±24             | 130±31             | <0.001  |
| MRI end-systolic volume, mL                            | 93±33         | 85±38              | 107±40             | 0.0078  |
| MRI end-systolic volume index, mL/m <sup>2</sup>       | 45±15         | 40±16              | 52±19              | 0.0104  |
| MRI ejection fraction, %                               | 61±6          | 61±7               | 61±6               | 0.82    |
| MRI LV mass, g   | 182±48        | 172±43             | 205±50             | <0.001  |
| MRI LV mass index, g/m <sup>2</sup>                    | 85±24         | 82±23              | 99±20              | <0.001  |
| MRI native T1 relaxation time, ms                      | 1020±30       | 1017±31            | 1025±29            | 0.12    |
| MRI extracellular volume fraction, %                   | 24±3          | 24±4               | 24±2               | 0.95    |
| Presence of myocardial scar, N (%)                     | 26 (20)       | 17 (21)            | 9 (22)             | 0.92    |
| <b>AR assessment</b>                                   |               |                    |                    |         |
| <b>Integrative approach</b>                            |               |                    |                    |         |
| AR grade IV, N (%)                                     | 59 (46)       | 34 (39)            | 25 (61)            | 0.0386  |
| 2D ECHO vena contracta width, mm                       | 6.3±1.5       | 6.1±1.6            | 6.6±1.5            | 0.11    |
| Diastolic flow reversal velocity, cm/s                 | 19±4          | 18±4               | 21±4               | <0.001  |
| 2D ECHO regurgitant volume, mL                         | 79±59         | 73±56              | 104±64             | 0.11    |
| 2D ECHO regurgitant fraction, %                        | 46±16         | 45±15              | 49±16              | 0.19    |
| 3D ECHO vena contracta area, mm <sup>2</sup> (92%)     | 29±12         | 25±13              | 34±14              | 0.0013  |
| MRI regurgitation volume, mL                           | 47±28         | 36±24              | 65±31              | <0.001  |
| MRI regurgitation fraction, %                          | 37±16         | 32±14              | 46±16              | <0.001  |

Values are means±SDs or numbers (percentage). 2D indicates 2-dimensional; 3D, 3-dimensional; AR, aortic regurgitation; ECHO, echocardiography; LV, left ventricle; and MRI, magnetic resonance imaging.

markers of diffuse myocardial fibrosis were similar. The end point group tended to have lower LV GLS ( $P=0.07$ ) and showed more impaired LV diastolic function ( $P<0.05$ ) than patients without end point (Table 2). We observed a higher prevalence of grade IV AR using an integrative approach, larger 3D VCA, MRI-derived RV, and RF of AR (all  $P<0.05$ ) in the end point group. Out of 41 patients with AV surgery indication, a total of 34 (83%) patients effectively underwent AV surgery, whereas in the remaining ones the surgery was postponed because of patients' refusal or epidemic. Twenty-one (62%) and 13 (38%)

patients, respectively, underwent isolated AV surgery and AV surgery plus concomitant aortic root replacement. The AV-sparing surgery was performed in 29% of individuals, while AVR using a bioprosthetic or mechanical valve in 29% or 32%, respectively, and the Ross procedure in 9%. The AV surgery was successful in all patients. Perioperative and 30-day mortality was 0. One patient died 6 months after AV replacement due to early prosthetic infective endocarditis. All the remaining patients were alive at the end of the follow-up. No patient needed redo AV surgery. A total of 32 (78%) surgically treated patients

underwent a follow-up MRI study analyzed in a CoreLab, which showed a significant LV reverse remodeling with a decrease in LVEDVI ( $123 \pm 31$  mL/m<sup>2</sup> vs  $78 \pm 23$  mL/m<sup>2</sup>;  $P < 0.001$ ), LV end-systolic volume index (LVESVI;  $48 \pm 19$  mL/m<sup>2</sup> vs  $36 \pm 13$  mL/m<sup>2</sup>;  $P < 0.001$ ), and LV mass index ( $98 \pm 22$  g/m<sup>2</sup> vs  $75 \pm 15$  g/m<sup>2</sup>;  $P < 0.001$ ).

### Predictors of Clinical Outcome

Figure 1 shows the association between selected parameters and end point using spline curve analysis. In general, indices related to AR assessment versus LV remodeling had a larger area under the curve to identify individuals with future end points (Table 3). In multivariable Cox

regression analysis, age, BNP, 3D VCA, MRI-derived LV end-diastolic volume index, RV, and RF were identified as independent predictors of end point (Table 4). However, a combined model including one parameter of AR assessment, one parameter of LV remodeling, and BNP showed significantly higher predictive accuracy than any single parameter alone. Using MRI-derived indices, the largest area under the curve was observed for a combination of either RV (Figure 2A) or RF (Figure 2B) with LVEDVI and BNP. Hazard ratio to predict end point significantly increased with 2 to 3 indices exceeding cutoff values (hazard ratio, 12.45 [95% CI, 2.9–53.38];  $P = 0.0012$ ) compared with only one parameter (hazard ratio, 3.81 [95% CI, 0.81–17.93];  $P = 0.09$ ). At echocardiography,

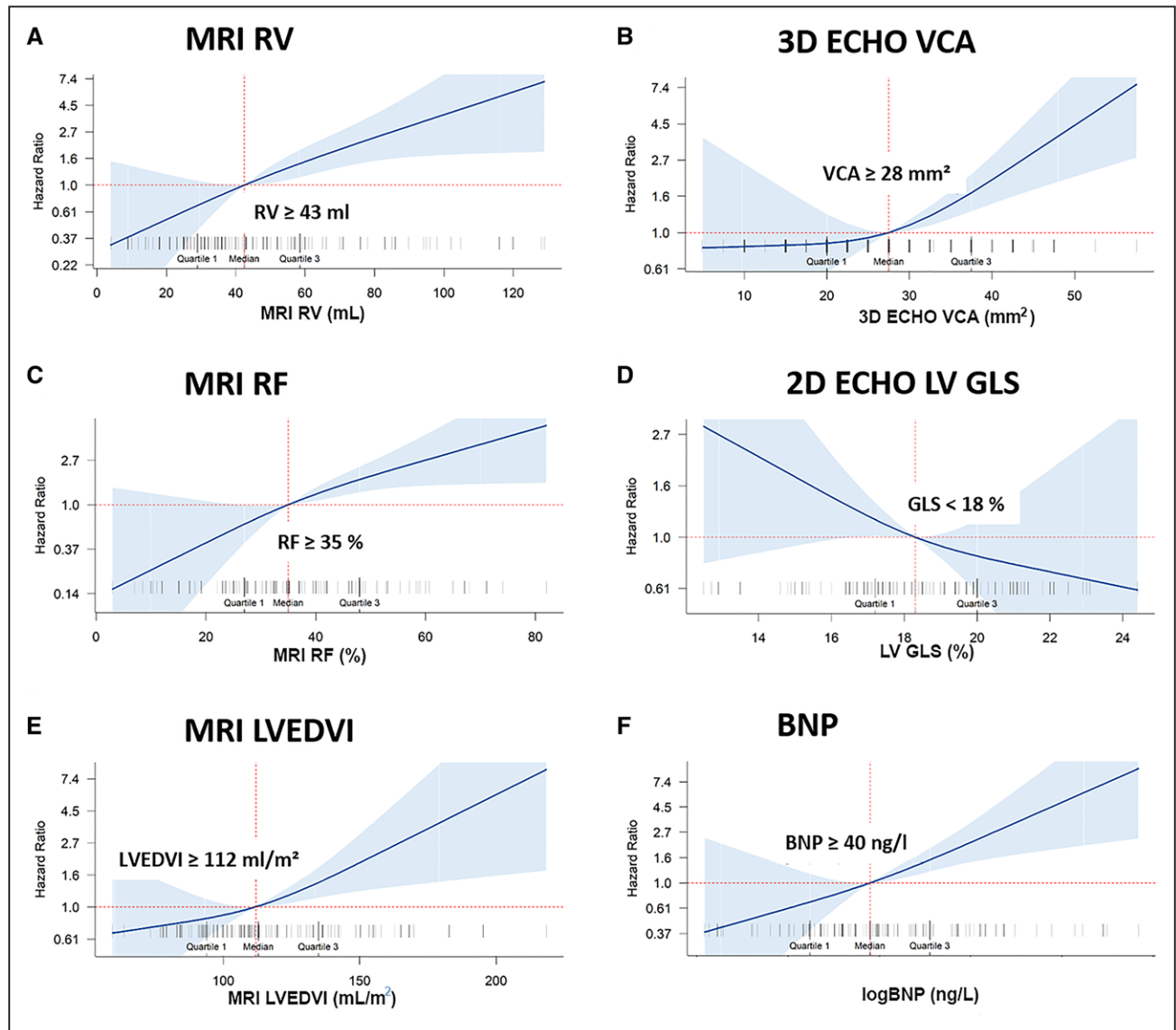


**Figure 1. Association between the onset of indication for aortic valve surgery.**

**A**, Magnetic resonance imaging (MRI)-derived regurgitant volume (MRI RV); **B**) 3-dimensional echocardiography-derived vena contracta area (3D ECHO VCA); **C**) MRI-derived regurgitant fraction (MRI RF); **D**) 2-dimensional echocardiography-derived left ventricular (LV) global longitudinal strain (2D ECHO LV GLS); **E**) MRI-derived LV end-diastolic volume index (MRI LVEDVI); **F**) Brain natriuretic peptide (BNP). Risk (hazard ratio) increased with MRI RV  $\geq 43$  ml, MRI RF  $\geq 35$ %, MRI LVEDVI  $\geq 112$  mL/m<sup>2</sup>, 3D ECHO VCA  $\geq 28$  mm<sup>2</sup>, 2D ECHO LV GLS  $< 18$ % and BNP  $\geq 40$  ng/l.

**Table 3. Predictive Accuracy of Selected Parameters to Identify Patients Who Developed AV Surgery Indication**

|                                   | AUC (95% CI)     | Cutoff value | Sensitivity, % | Specificity, % |
|-----------------------------------|------------------|--------------|----------------|----------------|
| Age, y                            | 0.61 (0.50–0.72) | 45           | 69             | 63             |
| BNP, ng/L                         | 0.71 (0.60–0.81) | 40           | 74             | 63             |
| ECHO LVEDVI, mL/m <sup>2</sup>    | 0.58 (0.45–0.71) | 92           | 41             | 80             |
| 2D ECHO GLS, %                    | 0.61 (0.49–0.73) | −17          | 34             | 84             |
| Transmitral E wave velocity, cm/s | 0.64 (0.53–0.75) | 57           | 50             | 75             |
| MRI LVEDVI, mL/m <sup>2</sup>     | 0.64 (0.51–0.76) | 124          | 59             | 74             |
| MRI LVESVI, mL/m <sup>2</sup>     | 0.61 (0.47–0.74) | 54           | 53             | 80             |
| MRI LVEDV, mL                     | 0.63 (0.51–0.75) | 252          | 59             | 66             |
| 2D ECHO integrative approach      | 0.59 (0.49–0.69) | Grade IV AR  | 59             | 58             |
| 3D VCA, mm <sup>2</sup>           | 0.66 (0.54–0.78) | 36           | 50             | 82             |
| MRI RV, mL                        | 0.71 (0.60–0.81) | 45           | 72             | 63             |
| MRI RF, %                         | 0.72 (0.62–0.82) | 34           | 78             | 57             |

2D indicates 2-dimensional; 3D, 3-dimensional; 3D VCA, 3D echocardiography VCA; AR, aortic regurgitation; AUC, area under the curve; AV, aortic valve; BNP, brain natriuretic peptide; ECHO, echocardiography; GLS, global longitudinal strain; LVEDV, left ventricle end-diastolic volume; LVEDVI, left ventricular end-diastolic volume index; LVESVI, left ventricular end-systolic volume index; MRI, magnetic resonance imaging; MRI LVEDVI, MRI-derived LV end-diastolic volume index; MRI RF, MRI-derived RF; MRI RV, MRI-derived RV; RF, regurgitant fraction; RV, regurgitant volume; and VCA, vena contracta area.

a combined model using 3D VCA, 2D GLS (Figure 3A), or transmitral E wave (Figure 3B), and BNP yielded the largest area under the curve, which was, nevertheless, smaller than that of the MRI-derived models. Figure 4 shows an example of the model combining MRI- and echocardiography-derived parameters with BNP.

### Validation in the External Test Cohort

The test cohort included 100 consecutive patients with 38 end points during a median follow-up of 1252 (interquartile range, 902–1534) days. The baseline characteristics between the derivation and the validation cohort were similar (Table S1). Performance of models combining MRI- and/or echocardiography-derived indices and natriuretic peptides to identify patients with early disease progression remained robust in the validation cohort (Table S2). MRI-based models showed higher

performance than echocardiography-derived models (AUC, 0.85–0.87 versus 0.72–0.75, respectively).

### Reproducibility

Intraobserver and interobserver reproducibility was tested on 10 randomly selected patients' echocardiography and MRI datasets for MRI-derived RV and RF, LVEDVI and LVESVI, 3D VCA, 2D VC width, GLS, native T1 relaxation time using intraclass correlation coefficient. The intraobserver and interobserver intraclass correlation coefficient, respectively, was >0.94 and >0.82 suggesting high reproducibility.

## DISCUSSION

In asymptomatic patients with severe AR, preserved LV EF, and LV end-systolic diameter, we have demonstrated

**Table 4. Independent Predictors of Aortic Valve Surgery Indication**

|                             | Univariable analysis |         | Multivariable analysis |         |
|-----------------------------|----------------------|---------|------------------------|---------|
|                             | HR (95% CI)          | P value | HR (95% CI)            | P value |
| Age                         | 1.05 (1.00–1.10)     | 0.0474  | 1.02 (0.93–1.12)       | 0.34    |
| Log BNP                     | 4.14 (2.05–8.35)     | 0.0098  | 4.67 (1.91–11.31)      | <0.001  |
| 2D GLS                      | 0.87 (0.75–1.00)     | 0.05    |                        |         |
| Transmitral E wave velocity | 0.98 (0.96–1.00)     | 0.05    |                        |         |
| 3D VCA                      | 1.05 (1.02–1.09)     | <0.001  | 1.04 (1.01–1.07)       | 0.0086  |
| MRI LVEDVI                  | 1.02 (1.01–1.03)     | 0.0043  | 1.01 (0.99–1.02)       | 0.55    |
| MRI RV                      | 1.02 (1.01–1.04)     | <0.001  | 1.02 (1.01–1.03)       | 0.0352  |
| MRI RF                      | 1.04 (1.02–1.06)     | <0.001  | 1.04 (1.01–1.06)       | 0.0071  |

2D indicates 2-dimensional; 3D VCA, 3-dimensional echocardiography vena contracta area; BNP, brain natriuretic peptide; GLS, global longitudinal strain; HR, hazard ratio; LVEDVI, left ventricular end-diastolic volume index; MRI, magnetic resonance imaging; MRI LVEDVI, MRI-derived LV end-diastolic volume index; MRI RF, MRI-derived RF; MRI RV, MRI-derived RV; RF, regurgitant fraction; and RV, regurgitant volume.

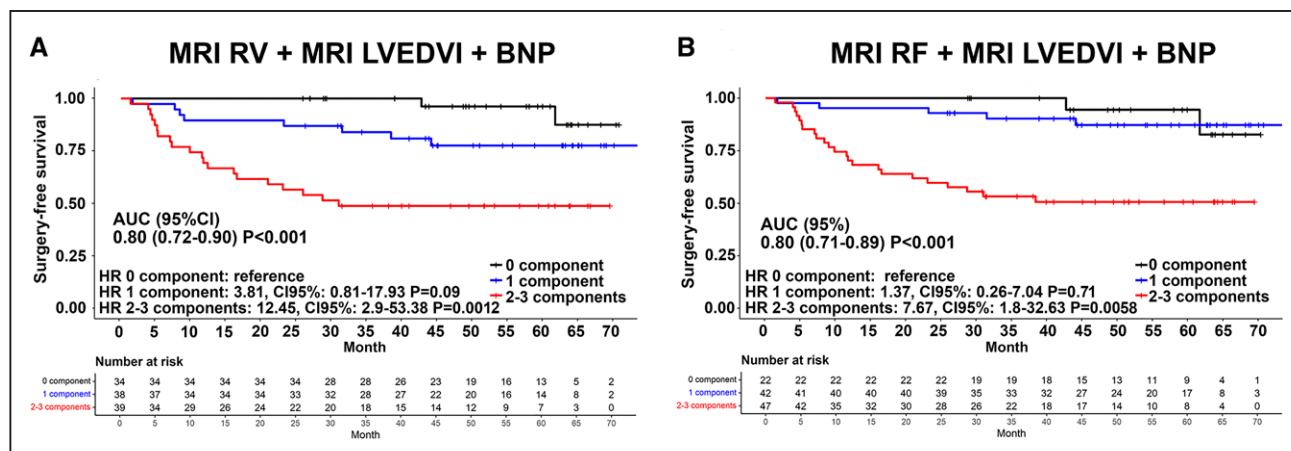


**Figure 2. Magnetic resonance imaging (MRI) model combining MRI-derived regurgitant volume (MRI RV; A) or regurgitant area under the curve (MRI RF; B), left ventricular end-diastolic volume index (LVEDVI) and BNP (brain natriuretic peptide) show a larger area under the curve than any single parameter alone (P<0.001).**

Hazard ratio (HR) to predict end point significantly increased with 2-3 parameters exceeding cutoff values, derive by using spline curve analysis, compared to any parameter alone. AUC indicates area under curve.

that the multiparametric strategy combining 2 imaging parameters, for example, one to quantify AR severity and another one to assess LV remodeling or subtle LV dysfunction, with natriuretic peptide showed higher accuracy than any parameter alone to identify individuals with early disease progression. In general, parameters of AR severity assessment performed better than indices of LV remodeling or function. Models involving either MRI alone or in combination with echocardiography plus natriuretic peptides showed higher accuracy than models including only echocardiography and natriuretic peptides. MRI showed added value mostly for AR quantification where it outperformed all standard echocardiography measurements with exception of 3D VCA, which is, however, not routinely used. These advocates for the more liberal implementation of MRI in an asymptomatic patient with severe AR at the early stage of the disease.

### Management of Severe AR

Chronic AR results in a combined volume and pressure overload of the LV<sup>17,18</sup> leading to LV dilatation, increase in LV mass and, if untreated, LV decompensation resulting in heart failure and/or premature death. In contrast, timely surgical treatment is associated with significant reverse remodeling and perhaps normalization of LV structure and function.<sup>19</sup> However, the currently recommended approach integrating echocardiography-derived AR quantification, LV EF, and LV end-systolic diameter is insensitive to identifying patients with early adverse clinical course.<sup>20,21</sup> This has been demonstrated by several large studies showing, in mainly asymptomatic patients with severe AR and normal LV EF, better both preoperative and postoperative survival in individuals with LV end-systolic diameter indexed (I) below the currently recommended threshold for AV intervention.<sup>10-12,20,22</sup> Corroborating these results,

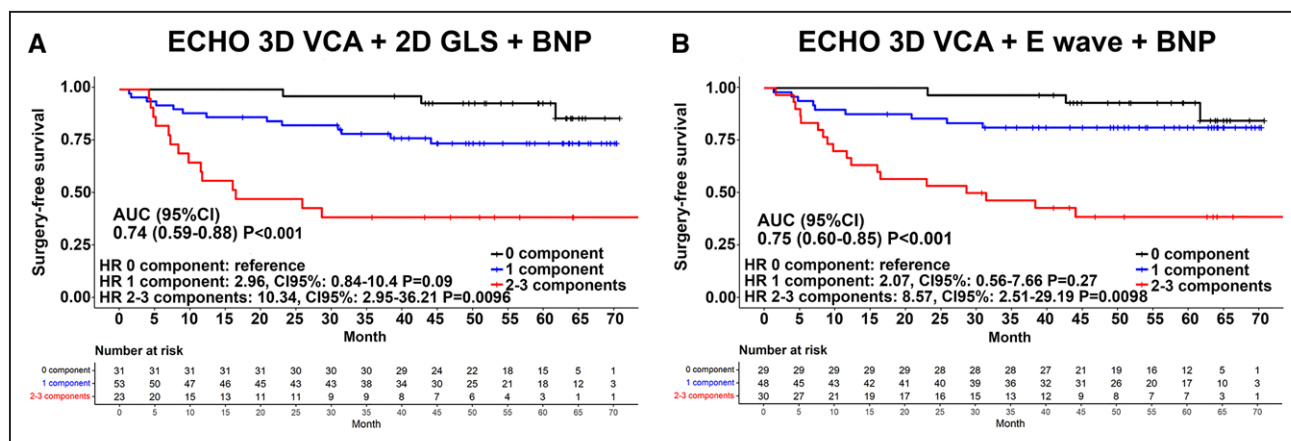


**Figure 3. Echocardiography (ECHO) model including ECHO-derived 3-dimensional vena contracta area (ECHO 3D VCA), 2-dimensional global longitudinal strain (2D GLS; A) or transmitral E wave (B) and BNP (brain natriuretic peptide) shows a larger area under the curve than any single parameter alone (P<0.001).**

Hazard ratio (HR) to predict end point significantly increased with 2-3 parameters exceeding cutoff values, derive by using spline curve analysis, compared to any parameter alone. AUC indicates area under curve.

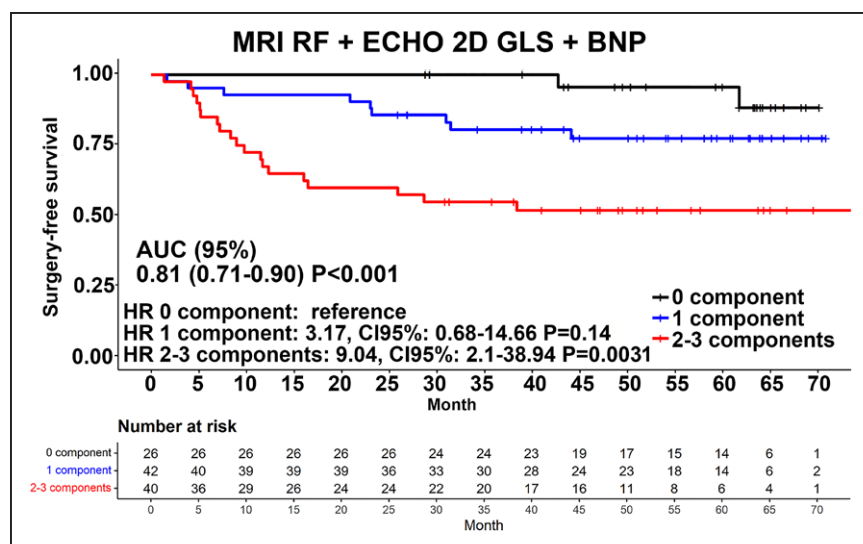


**Figure 4. Multimodality model including magnetic resonance imaging–derived regurgitant fraction (MRI RF), 2- dimensional echocardiography-derived global longitudinal strain (ECHO 2D GLS) and BNP (brain natriuretic peptide).** AUC indicates area under curve; and HR, hazard ratio.

in the present study, a significant proportion of asymptomatic patients with normal LV EF and ESDI <25 mm/m<sup>2</sup> developed symptoms during relatively a short time. Patients with early disease decompensation had a higher prevalence of grade IV AR per echocardiography integrative approach with a relatively low area under the curve of 0.59 to predict end point. In contrast, MRI-derived RF (AUC, 0.72) and 3D echocardiography VCA (AUC, 0.66) showed the highest accuracy to predict the onset of AV surgery indication. Consistently with previously published data of Myerson et al,<sup>3</sup> Harris et al,<sup>23</sup> and Vejpongsa et al,<sup>24</sup> the prognostically valuable thresholds of MRI-derived RV >45 mL and RF >34% were much lower (Myerson RV >42 mL, RF >33%; Harris RV >50 mL, RF ≥37%; and Vejpongsa RF >35%)<sup>3,23,24</sup> than traditional echocardiography cut off values of severe AR (RV ≥60 mL, RF ≥50%).<sup>6,14</sup> Indices of LV remodeling, both at echocardiography and MRI, had lower predictive accuracy (AUC, 0.58–0.64) to identify early disease decompensation probably reflecting the very early AR stage in our study. In recent studies, myocardial scar, GLS, increased ECV index for body surface area, and BNP have been associated with the early adverse course of reduced survival before or after AV surgery.<sup>7,13,24–28</sup> These markers showed a relatively low predictive value in our patient group comprising a rather younger population with fewer comorbidities at early disease stage. Yet, we observed impaired GLS, diastolic function, the more frequent presence of myocardial scar in late gadolinium enhancement, lower values of T1 relaxation time, and increased BNP in patients with end points implying subtle myocardial damage. In addition, in the present study, 24 patients who underwent a perioperative myocardial biopsy, showed an increased extent of myocardial fibrosis of 16±7%, whereas the normal range is 1% to 7%.<sup>19,29,30</sup> Thus, optimal timing of AV intervention is crucial to prevent irreversible changes and to achieve an optimal long-term outcome. In this regard, single indices of AR quantification showed independent predictive

value to identify the onset of symptoms or LV dysfunction, yet their performance remains suboptimal (AUC, 0.72) to guide clinical decision-making between early intervention or watchful waiting strategy. Therefore, a combination of several indices may provide more robust results. In the present study, a simple model including 3 parameters showed a significantly larger area under the curve to predict the end point than any single parameter alone. This suggests that a multiparametric strategy may improve risk stratification in the early stage of AR and facilitate patient management.

### Limitations

Cardiac MRI showed the best predictive accuracy out of all tested imaging and biochemical markers in the present study. However, we have to admit that this cardiac imaging method is not routinely available to all cardiology centers. The method is costly and requires expertise and tight collaboration of technologists, cardiologists, and radiologists.

The majority of patients were under 50 years of age, and 71% had a bicuspid AV with frequently presented an eccentric regurgitant jet making the conventional echocardiography AR quantification difficult. This might explain that the best predictive echocardiography marker was 3D VCA instead of traditional echocardiography parameters. Moreover, 3D VCA is not routinely measured in clinical practice and requires a certain level of expertise. However, both availability of MRI/3D echocardiography equipment and expertise within heart valve centers is growing. Thus, these limitations may not significantly hamper the generalizability of these results.

### Conclusions

Asymptomatic patients with severe AR, not yet fulfilling guidelines indication for AV intervention, may be at

risk of early disease decompensation. This suggests that the current approach integrating echocardiography-derived AR assessment and LV remodeling is rather insensitive to detecting individuals in need of early AV intervention. In the present study, multimodality and multiparametric model consisting of 3 indices, i.e., one parameter of MRI-derived AR quantification plus one parameter of either MRI- or echocardiography-derived LV dilatation or dysfunction, plus natriuretic peptides, showed high accuracy to identify early disease decompensation. The performance of these models remained robust also in the external validation cohort. This suggests that MRI assessment should be implemented in eligible patients with asymptomatic moderate or severe AR to facilitate clinical decision-making between early AV intervention versus watchful waiting with regular visits at the valve clinic.

## ARTICLE INFORMATION

Received September 22, 2022; accepted November 7, 2022.

### Affiliations

Cardiothoracic Surgery Department, Na Homolce Hospital, Czech Republic (R.K., I.S., S.C.). Department of Cardiology, Royal Vinohrady University Hospital, Czech Republic (H.L.). Department of Cardiology (Z.H.) and Department of Cardiovascular Surgery (J.H.), General University Hospital, Prague, Czech Republic. 1st Department Medicine - Cardioangiology, University Hospital Hradec Králové, Sokolská Czech Republic (K.M.). Department of Cardiac Surgery, University Hospital Hradec Králové, Hradec Králové, Czech Republic (M.T., J.V.). Institute for Clinical and Experimental Medicine, Prague, Czech Republic (J.M.). Cardiovascular Center Aalst, Belgium (T.M., C.D.C., M.P.). Division of Clinical Pharmacology, Department of Pharmacology, Showa University, Tokyo, Japan (T.M.). Department of Advanced Biomedical Sciences, University Federico II, Naples, Italy (C.D.C.).

### Acknowledgments

We are grateful to Dr Marek Malý (National Institute of Public Health, Prague, Czech Republic) for the statistical analysis, and to Prof. David Sedmera (First Faculty of Medicine, Institute of Anatomy, Charles University in Prague) and Matěj Kočka (Medical student of Trinity College Dublin, Ireland) for their invaluable myocardial histology analysis.

### Sources of Funding

This study was supported by the Ministry of Health of the Czech Republic 17-28265A.

### Disclosures

None.

### Supplemental Material

Tables S1–S2

## REFERENCES

- Baumgartner H, Falk V, Bax JJ, De Bonis M, Hamm C, Holm RJ, Jung B, Lancellotti P, Lansac E, Rodriguez Muñoz D, et al. 2017 ESC/EACTS Guidelines for the management of valvular heart disease. *Eur Heart J*. 2017;38:2739–2791. doi: 10.1093/eurheartj/ehx391
- Jung B. A prospective survey of patients with valvular heart disease in Europe: the Euro Heart Survey on Valvular Heart Disease. *Eur Heart J*. 2003;24:1231–1243. doi: 10.1016/s0195-668x(03)00201-x
- Myerson SG, d'Arcy J, Mohiaddin R, Greenwood JP, Karamitsos TD, Francis JM, Banning AP, Christiansen JP, Neubauer S. Aortic regurgitation quantification using cardiovascular magnetic resonance: association with clinical outcome. *Circulation*. 2012;126:1452–1460. doi: 10.1161/CIRCULATIONAHA.111.083600
- Nishimura RA, Otto CM, Bonow RO, Carabello BA, Erwin JP, Fleisher LA, Jneid H, Mack MJ, McLeod CJ, O'Gara PT et al. 2017 AHA/ACC Focused Update of the 2014 AHA/ACC guideline for the management of patients with valvular heart disease: a report of the American College of Cardiology/American Heart Association task force on clinical practice guidelines. *Circulation*. 2017;135:e1159–e1195. doi: 10.1161/CIR.0000000000000503
- Nkomo VT, Gardin JM, Skelton TN, Gottdiener JS, Scott CG, Enriquez-Sarano M. Burden of valvular heart diseases: a population-based study. *Lancet*. 2006;368:1005–1011. doi: 10.1016/S0140-6736(06)69208-8
- Steeds RP, Myerson SG. Imaging assessment of mitral and aortic regurgitation: current state of the art. *Heart*. 2020;106:1769–1776. doi:10.1136/heartjnl-2019-316216
- Alashi A, Khullar T, Mentias A, Gillinov AM, Roselli EE, Svensson LG, Popovic ZB, Griffin BP, Desai MY. Long-term outcomes after aortic valve surgery in patients with asymptomatic chronic aortic regurgitation and preserved left ventricular function and follow-up global longitudinal strain. *JACC Cardiovasc Imaging*. 2020;13:12–21. doi: 10.1016/j.jcmg.2018.12.021
- Desai MY. Aortic regurgitation: are we operating too late? *Ann Cardiothorac Surg*. 2019;8:39092–39392. doi: 10.21037/acs.2019.0
- Dujardin KS, Enriquez-Sarano M, Schaff HV, Bailey KR, Seward JB, Tajik AJ. Mortality and morbidity of aortic regurgitation in clinical practice. A long-term follow-up study. *Circulation*. 1999;99:1851–1857. doi: 10.1161/01.cir.99.14.1851
- de Meester C, Gerber BL, Vancaeynest D, Pouleur A-C, Noirhomme P, Pasquet A, de Kerchove L, El Khoury G, Vanoverschelde J-L. Do guideline-based indications result in an outcome penalty for patients with severe aortic regurgitation? *JACC Cardiovasc Imaging*. 2019;12:2126–2138. doi: 10.1016/j.jcmg.2018.11.022
- Mentias A, Feng K, Alashi A, Rodriguez LL, Gillinov AM, Johnston DR, Sabik JF, Svensson LG, Grimm RA, Griffin BP, et al. Long-term outcomes in patients with aortic regurgitation and preserved left ventricular ejection fraction. *J Am Coll Cardiol*. 2016;68:2144–2153. doi: 10.1016/j.jacc.2016.08.045
- Yang L-T, Michelena HI, Scott CG, Enriquez-Sarano M, Pislaru SV, Schaff HV, Pellikka PA. Outcomes in chronic hemodynamically significant aortic regurgitation and limitations of current guidelines. *J Am Coll Cardiol*. 2019;73:1741–1752. doi: 10.1016/j.jacc.2019.01.024
- Malahfi M, Senapati A, Tayal B, Nguyen DT, Graviss EA, Nagueh SF, Reardon MJ, Quinones M, Zoghbi WA, Shah DJ. Myocardial scar and mortality in chronic aortic regurgitation. *J Am Heart Assoc*. 2020;9:e018731. doi: 10.1161/JAHA.120.018731
- Zoghbi WA, Adams D, Bonow RO, Enriquez-Sarano M, Foster E, Grayburn PA, Hahn RT, Han Y, Hung J, Lang RM, et al. Recommendations for noninvasive evaluation of native valvular regurgitation: a report from the American Society of Echocardiography developed in collaboration with the Society for Cardiovascular Magnetic Resonance. *J Am Soc Echocardiogr*. 2017;30:303–371. doi: 10.1016/j.echo.2017.01.007
- Kočková R, Linková H, Hlubocká Z, Pavečková A, Polednová A, Sůkupová L, Bláha M, Malý J, Honsová E, Sedmera D, et al. New imaging markers of clinical outcome in asymptomatic patients with severe aortic regurgitation. *J Clin Med*. 2019; 8:1654. doi: 10.3390/jcm8101654
- Kockova R, Kacer P, Pirk J, Maly J, Sukupova L, Sikula V, Kotrc M, Barciakova L, Honsova E, Maly M, et al. Native T1 relaxation time and extracellular volume fraction as accurate markers of diffuse myocardial fibrosis in heart valve disease - comparison with targeted left ventricular myocardial biopsy. *Circ J*. 2016;80:1202–1209. doi: 10.1253/circj.CJ-15-1309
- Lee JK, Franzone A, Lanz J, Siontis GC, Stortecky S, Grani C, Roost E, Windecker S, Pilgrim T. Early detection of subclinical myocardial damage in chronic aortic regurgitation and strategies for timely treatment of asymptomatic patients. *Circulation*. 2018;137:184–196. doi: 10.1161/CIRCULATIONAHA.117.0298
- Carabello BA. The relationship of left ventricular geometry and hypertrophy to left ventricular function in valvular heart disease. *J Heart Valve Dis*. 1995;4 Suppl 2:S132–138; discussion S138–139. doi: 10.1291/hypres.25.191
- Krayenbuehl HP, Hess OM, Monrad ES, Schneider J, Mall G, Turina M. Left ventricular myocardial structure in aortic valve disease before, intermediate, and late after aortic valve replacement. *Circulation*. 1989;79:744–755. doi: 10.1161/01.cir.79.4.744
- Vahanian A, Beyersdorf F, Praz F, Milojevic M, Baldus S, Bauersachs J, Capodanno D, Conradi L, De Bonis M, De Paulis R, et al. 2021 ESC/EACTS guidelines for the management of valvular heart disease. *Eur Heart J*. 2022;43:561–632. doi: 10.1093/eurheartj/ehab395

21. Otto CM, Nishimura RA, Bonow RO, Carabello BA, Erwin JP, Gentile F, Jneid H, Krieger EV, Mack M, McLeod C, O'Gara PT, Rigolin VH, Sundt TM, Thompson A, Toly C. 2020 ACC/AHA guideline for the management of patients with valvular heart disease: a report of the American College of Cardiology/American Heart Association Joint Committee on Clinical Practice Guidelines. *Circulation*. 2021;143:e72–e227. doi: 10.1161/CIR.0000000000000923
22. Detaint D, Messika-Zeitoun D, Maalouf J, Tribouilloy C, Mahoney DW, Tajik AJ, Enriquez-Sarano M. Quantitative echocardiographic determinants of clinical outcome in asymptomatic patients with aortic regurgitation: a prospective study. *JACC Cardiovasc Imaging*. 2008;1:1–11. doi: 10.1016/j.jcmg.2007.10.008
23. Harris AW, Krieger EV, Kim M, Cawley PJ, Owens DS, Hamilton-Craig C, Maki J, Otto CM. Cardiac magnetic resonance imaging versus transthoracic echocardiography for prediction of outcomes in chronic aortic or mitral regurgitation. *Am J Cardiol*. 2017;119:1074–1081. doi: 10.1016/j.amjcard.2016.12.017
24. Vejpongsa P, Xu J, Quinones MA, Shah DJ, Zoghbi WA. Differences in cardiac remodeling in left-sided valvular regurgitation. *JACC Cardiovasc Imaging*. 2022;15:1730–1741. doi: 10.1016/j.jcmg.2022.05.006
25. Kammerlander AA, Wiesinger M, Duca F, Aschauer S, Binder C, Zotter Tufaro C, Nitsche C, Badre-Eslam R, Schönbauer R, Bartko P, et al. Diagnostic and prognostic utility of cardiac magnetic resonance imaging in aortic regurgitation. *JACC Cardiovasc Imaging*. 2019;12:1474–1483. doi: 10.1016/j.jcmg.2018.08.036
26. Weber M, Hausen M, Arnold R, Moellmann H, Nef H, Elsaesser A, Mitrovic V, Hamm C. Diagnostic and prognostic value of N-terminal pro B-type natriuretic peptide (NT-proBNP) in patients with chronic aortic regurgitation. *Int J Cardiol*. 2008;127:321–327. doi: 10.1016/j.ijcard.2007.07.174
27. Pizarro R, Bazzino OO, Oberti PF, Falconi ML, Arias AM, Krauss JG, Cagide AM. Prospective validation of the prognostic usefulness of b-type natriuretic peptide in asymptomatic patients with chronic severe aortic regurgitation. *J Am Coll Cardiol*. 2011;58:1705–1714. doi: 10.1016/j.jacc.2011.07.016
28. Senapati A, Malahfji M, Debs D, Yang EY, Nguyen DT, Graviss EA, Shah DJ. Regional replacement and diffuse interstitial fibrosis in aortic regurgitation. *JACC Cardiovasc Imaging*. 2021;14:2170–2182. doi: 10.1016/j.jcmg.2021.04.028
29. Tanaka M, Fujiwara H, Onodera T, Wu DJ, Hamashima Y, Kawai C. Quantitative analysis of myocardial fibrosis in normals, hypertensive hearts, and hypertrophic cardiomyopathy. *Br Heart J*. 1986;55:575–581. doi: 10.1136/hrt.55.6.575
30. Meckel CR, Wilson JE, Sears TD, Rogers JG, Goaley TJ, McManus BM. Myocardial fibrosis in endomyocardial biopsy specimens: do different biopsies affect estimation? *Am J Cardiovasc Pathol*. 1989;2:309–313. PMID: 2789804